ELSEVIER

Polymer 41 (2000) 3057–3068

polymer

Weld line strength of poly(vinyl chloride)/polyethylene blends

D. Jarus[a], J.W. Summers[b], A. Hiltner[a,*], E. Baer[a]

[a]*Department of Macromolecular Science and Center for Applied Polymer Research, Case Western Reserve University, Cleveland, OH 44106-7202, USA*
[b]*The Geon Company, Avon Lake, OH 44012, USA*

Received 23 December 1998; accepted 25 June 1999

Abstract

Stress–strain behavior coupled with fractography was used to investigate the weld line strength of 30/70 w/w poly(vinyl chloride)/high density polyethylene (PVC/HDPE) blends. The weld line strength determined in uniaxial tension depended upon the domain shape of the PVC phase at the weld line, with elongated domains causing weld line weakness. To alter the PVC domain shape, the viscosity ratio (η_{PVC}/η_{HDPE}) of the blend was varied by changing the PVC molecular weight. The domain shape at the fracture initiation site was used in conjunction with a modified Nielsen approach to predict the ductile to brittle transition at the weld line. For the composition studied, a critical aspect ratio of the PVC phase of 1.24 was determined. Elongation of the PVC domains above this critical value led to brittle weld lines. The domain shape at the weld line was modeled by a Taylor analysis of droplet deformation in an elongational flow field. The calculations predicted that a viscosity ratio of 21 would produce a particle with an aspect ratio of 1.24. The observed weld line strength confirmed this prediction: blends with a viscosity ratio below 21 were brittle, and those with a viscosity ratio above 21 had ductile weld lines. © 2000 Elsevier Science Ltd. All rights reserved.

Keywords: Weld line; Blend morphology; Viscosity ratio

1. Introduction

Poor weld line strength is a characteristic of injection molded blends of immiscible polymers [1,2]. The weak weld line strength derives from the flow-induced morphology at the weld line, which is different from the bulk. Specifically, the domains are usually elongated and oriented parallel to the weld line [3,4]. Methods exist to minimize the detrimental effects of the weld lines. One technique is to oscillate the flow across the weld line to alter the domain orientation. This requires very specialized equipment [5]. The most common technique is to design the mold so that the weld line occurs in a region that is expected to experience low stress [1]. This approach often requires a complex mold design.

Methods to achieve stronger weld lines in immiscible blends without special molding techniques or mold designs would be advantageous. The key is elimination of the elongated domains at the weld line. The viscosity ratio of the blend components controls the elongation of the dispersed phase at the weld line. When the viscosity of the dispersed phase is lower than that of the matrix, elongation of the dispersed phase is highly pronounced. The elongation decreases as the dispersed phase viscosity is increased above that of the matrix [6]. Although it has been suggested that increasing the viscosity of the dispersed phase to prevent elongation would be beneficial to weld line strength [7], it appears that no quantitative study of this effect has been performed.

Blends of poly(vinyl chloride) (PVC) and high density polyethylene (HDPE) are a good model system for a weld line study for several reasons. First, PVC is available in a broad range of molecular weights with similar polydispersities, and therefore a broad range of viscosities. Furthermore, due to its hierarchical particulate structure [8,9], PVC disperses well (prior to fusion) without the need for a compatibilizer. As the matrix, HDPE is a ductile material that undergoes considerable strain hardening, which allows it to support loads substantially greater than the yield stress. Therefore, HDPE is not easily embrittled by the addition of a second phase [10]. In addition, the weld line strength of HDPE is inherently strong, and is not greatly affected by common molecular causes of weld line weakness such as molecular orientation or low entanglement density [11]. Therefore the weld line strength of the blends is predominately controlled by the micro-scale phase morphology.

The PVC/HDPE blends are attractive for other

* Corresponding author. Tel.: +1-216-368-4186; fax: +1-216-368-6329.
E-mail address: pah6@po.cwru.edu (A. Hiltner).

0032-3861/00/$ - see front matter © 2000 Elsevier Science Ltd. All rights reserved.
PII: S0032-3861(99)00470-X

reasons. Unless blended with significant amounts of a flame-retardant additive, HDPE is very flammable. Because PVC is inherently flame retardant, it can be an alternative, inexpensive flame retardant for HDPE. Lastly, both polymers are sold in high volumes and portions are found in the recycle stream. Blends of PVC/HDPE from recycled materials would reduce environmental costs.

The goal of this study was to understand the relationship between the morphology and failure mechanisms of weld lines. A predictive model for the weld line strength based on the effect of viscosity ratio on the morphology and fracture mechanism was developed.

2. Experimental

2.1. Materials

Poly(vinyl chloride) (PVC) was provided by the Geon Company in the form of powder in a range of molecular weights (M_w) from 32,000 to 141,000, all with a polydispersity close to two, Table 1. High density polyethylene (HDPE) (Dow 04452N) was provided in the form of pellets by The Dow Chemical Company and had a MFI of 4.0. A lubricant, stearic acid, and Mark 1900, a dimethyl tin 2-ethylhexyl thioglycolate stabilizer supplied by Witco, were added for the PVC.

Shear viscosities of PVC compounded with 1.5 phr stabilizer and 1 phr lubricant, and HDPE as-received were determined on an Instron Capillary Rheometer Model 4204 according to ASTM D3835. The shear rate range was 3–3000 s^{-1}.

Table 1
Poly(vinyl chloride) resins

Trade name	Molecular weight (M_w)
Experimental	32,000
Geon 110 × 477[a]	43,000
Geon 110 × 334	56,000
Geon 100C13	67,000
Geon 27	83,000
Geon 30[a]	93,000
Geon 141	141,000

[a] Used only for viscosity measurements.

2.2. Processing

The materials were dry mixed in the proportions of 30 parts by weight PVC, 70 parts HDPE with 0.2 parts and 0.5 parts lubricant and stabilizer, respectively. The mix was melt blended on a Banbury mixer at 165°C for 5 min and immediately roll milled on a Farrel roll mill at 165°C for 5 min. The low blending temperature was intended to minimize fusion of the PVC particles and enhance dispersion. After milling, the blends were cubed for injection molding. Tensile bars (ASTM D 638) were molded on a Van Dorn

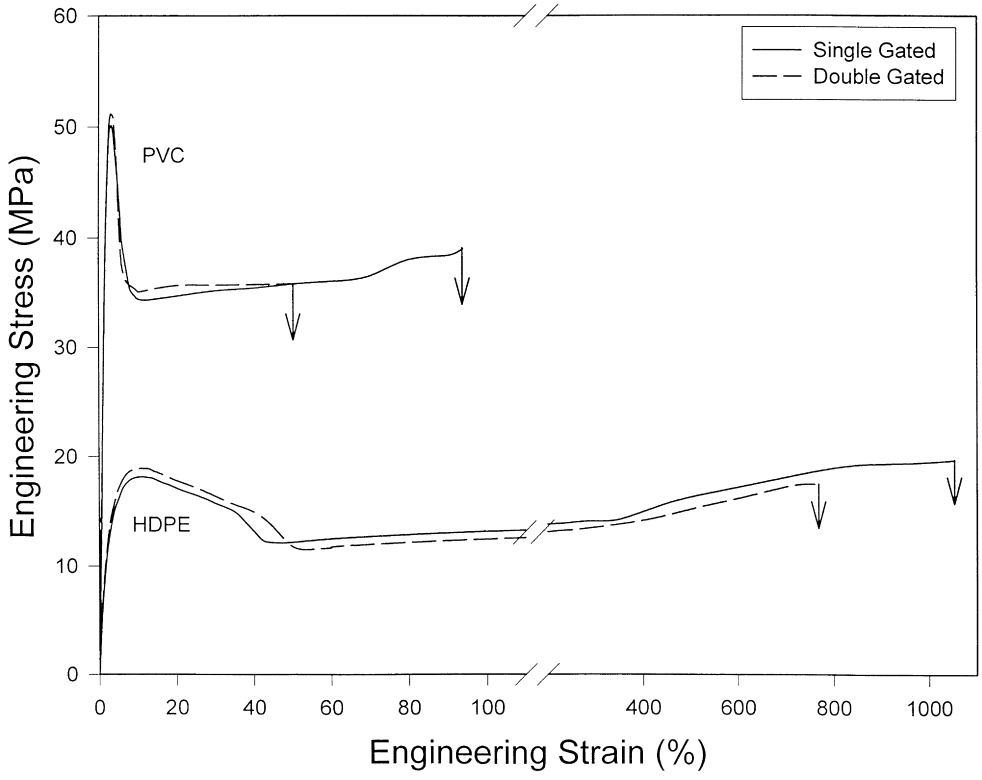

Fig. 1. Engineering stress–strain curves of HDPE and PVC with and without a weld line.

Table 2
Mechanical properties of components and blends

	Modulus (GPa)	Yield stress (MPa)	Yield strain (%)	Fracture strain (%)
PVC ($M_w = 56,000$)	3.10 ± 0.05	50 ± 1.0	3.2 ± 0.1	96 ± 6
HDPE	1.25 ± 0.05	18.1 ± 0.2	11.0 ± 0.4	1080 ± 30
Blends 30/70 PVC/HDPE				
PVC $M_w = 32,000$	1.86 ± 0.05	24.3 ± 0.2	6.4 ± 0.2	223 ± 42
PVC $M_w = 56,000$	1.84 ± 0.05	19.6 ± 0.3	5.9 ± 0.3	247 ± 22
PVC $M_w = 67,000$	1.61 ± 0.05	16.8 ± 0.4	4.9 ± 0.3	170 ± 15
PVC $M_w = 83,000$	1.56 ± 0.05	15.3 ± 0.2	3.6 ± 0.2	137 ± 19
PVC $M_w = 141,000$	1.53 ± 0.05	16.4 ± 0.3	4.0 ± 0.2	46 ± 9

75-ton injection-molding machine with either a single (no weld line) or double end-gated (weld line) configuration. Double end-gated bars were used as a worst case scenario for weld line formation. The barrel temperature was 190°C, the mold temperature was 40°C, the back pressure was 700 kPa, and the melt temperature was 200 ± 3°C.

2.3. Characterization

A 2 cm section was cut from an undeformed double-gated tensile bar to include the weld line. The section was notched on each of the cut surfaces with a razor blade, placed in liquid nitrogen for one hour, and then fractured lengthwise through the weld line. The domain morphology in the vicinity of the intact weld line was examined using a JEOL JSM-840A scanning electron microscope (SEM) after coating with 90 Å of gold. The anisotropy of the domain shapes was analyzed using an Optimas Image Analysis System. The aspect ratio of the domains was determined as the ratio of the long axis (l) to the short axis (w). Measurements of the aspect ratio were taken within 15 μm of the weld line. Although the particles were disk-shaped, the aspect ratio was measured in one plane. The aspect ratio in the third dimension was assumed to be the same. Domains of the lowest molecular weight PVC could not be characterized with this method because preparation always resulted in catastrophic fracture at the weld line and a section containing the intact weld line could not be isolated from the tensile bar.

Single and double end-gated tensile bars ($n = 5$) were tested on an Instron 1123 Universal Testing Machine to determine the uniaxial engineering stress–strain properties. The samples were tested at a strain rate of 5%/min.

After the double-gated specimens were tested, a 1 cm length section that included the fracture surface was

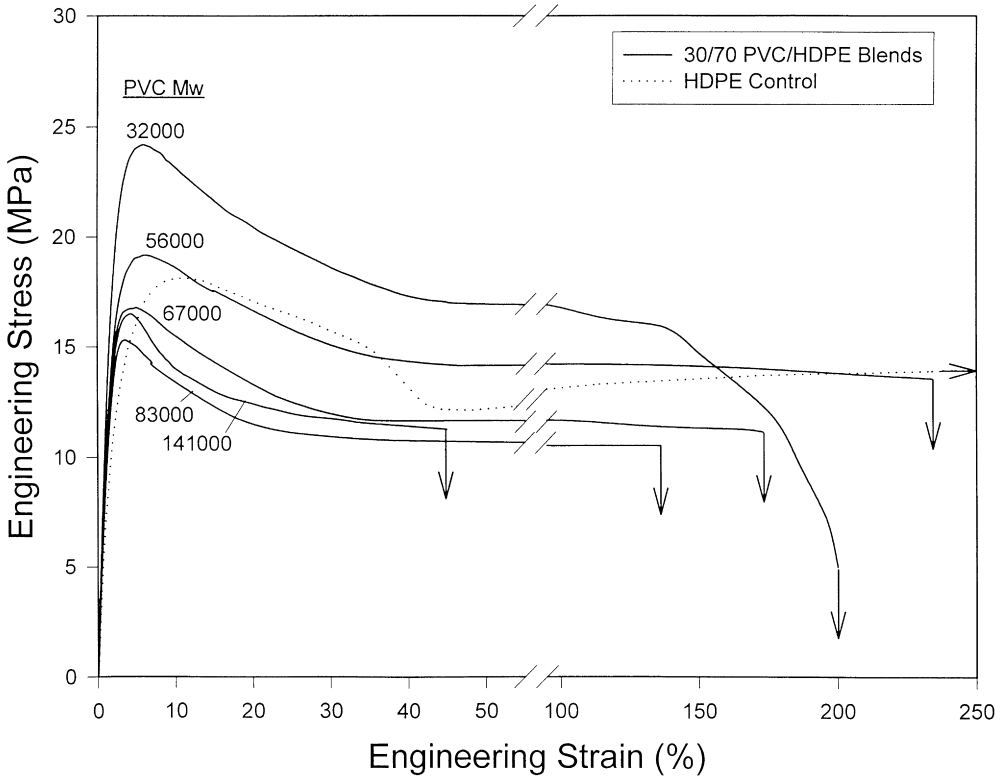

Fig. 2. Engineering stress–strain curves of 30/70 PVC/HDPE blends without weld line.

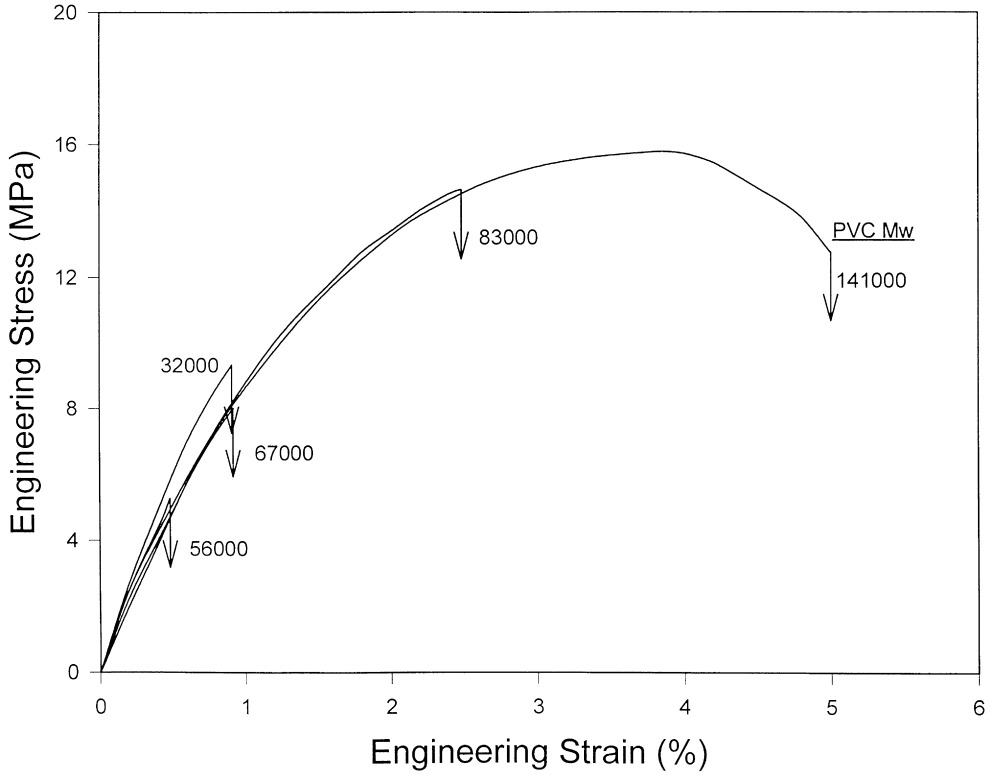

Fig. 3. Engineering stress–strain curves of 30/70 PVC/HDPE blends with a weld time.

sectioned from the tensile bar. The fracture surface was gold coated and viewed with SEM. After the fracture surface was examined, the specimen was notched on the cut face, opposite the fracture surface, and cryo-fractured as described previously. After gold coating, the morphology perpendicular to the fracture surface was examined in the SEM.

3. Results and discussion

3.1. Mechanical properties

The engineering stress–strain curves of HDPE and PVC are shown in Fig. 1. The modulus, yield stress and strain, and fracture strain for each material are listed in Table 2. Both materials deformed by local yielding and necking as suggested by the peak in engineering stress. The PVC yielded at 3% strain and immediately formed a sharp, well-defined neck profile. The draw ratio in the neck remained constant at about 2 as the neck propagated. Fracture occurred when the neck reached the end of the gauge section. In contrast, HDPE began to neck at about 11% strain and the diffuse neck gradually thinned until a well-defined neck profile was achieved at about 40% strain. The necked region of HDPE continued to draw as the neck propagated, achieving a draw ratio in excess of 10 at fracture.

When a weld line was introduced, PVC typically yielded away from the weld line and began to draw, however fracture always occurred when the propagating neck reached the weld line. The weld line could not support the large increase in local stress and strain. This reflected the inherent weakness of the weld line combined with the poor strain hardening characteristics of the PVC. In contrast, a weld line in HDPE did not prevent the neck from drawing through the entire gauge section. When the neck reached the weld line, even though the local stress and strain increased by a larger factor than in PVC, the ability of HDPE to strain harden compensated for any inherent weld line weakness. Furthermore, the weld line remained intact even though the edges started to separate after several hundred percent strain. This separation initiated at small, v-shaped notches about 5 μm deep at the weld line that formed during molding. Catastrophic fracture at the weld line did not occur until the strain exceeded 700% strain.

The engineering stress–strain curves of PVC/HDPE blends without a weld line are shown in Fig. 2. Because HDPE was the continuous phase, the modulus and yield stress were of the same magnitude as the HDPE values, Table 2. Blending with lower molecular weight PVC increased the yield stress above HDPE and blending with higher molecular weight PVC decreased the yield stress below HDPE. In general, the modulus, yield stress and strain, and fracture strain of the blends all decreased as the PVC molecular weight increased. Regardless of the molecular weight, all blends necked and began to draw.

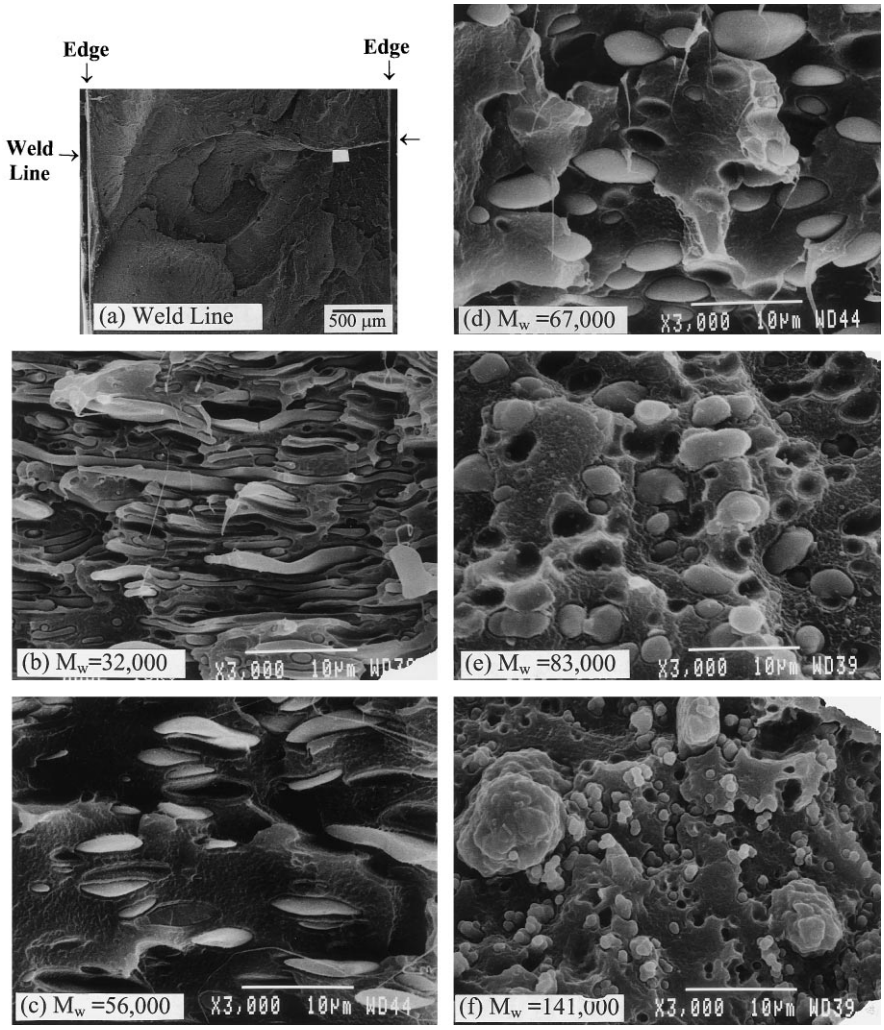

Fig. 4. (a) An unbroken weld line ($M_w = 67,000$) depicting the oxbow profile. Magnifications of the domain morphology as a function of PVC molecular weight at the location marked by the white box in (a); (b) $M_w = 32,000$; (c) $M_w = 56,000$; (d) $M_w = 67,000$; (e) $M_w = 83,000$; and (f) $M_w = 141,000$.

Yielding in the blends occurred at a much lower strain than in HDPE, and a well-defined neck profile formed rapidly. As the neck propagated, the necked region continued to thin and eventually fractured before the entire gauge section necked. The fracture strain decreased considerably compared to HDPE, but was generally higher than PVC.

When a weld line was introduced, fracture at the weld line decreased the fracture strain substantially. The trend toward lower fracture strain with increasing molecular weight reversed when a weld line was introduced, Fig. 3. Increasing the molecular weight of the PVC increased both the fracture stress and strain of the double-gated specimens, in contrast to the trend in specimens without a weld line. However, in all cases, the weld line dramatically reduced the fracture strain. In fact, blends with lower molecular weight PVC were brittle and fractured at the weld line before a neck formed. As the PVC molecular weight increased from 67,000 to 83,000 the blend almost reached the yield stress. The blend with a PVC molecular weight of 141,000 did reach the yield stress and began to neck at the weld line. Fracture occurred as the cross section began to thin.

3.2. Blend morphology at the weld line

Weld lines are created by the impingement of two opposing fountain flows. The instability created by this impingement determines the macroscopic weld line profile. Although the instability is not well understood, the shape of weld lines has been described as planar (no distortion), curved (first order distortion), or oxbow (second-order distortion) [12]. In this study, weld line profiles were always oxbow-shaped, Fig. 4(a). Blends with PVC molecular weights of 56,000, 67,000 and 83,000 had identical oxbow profiles. The blend with a molecular weight of 32,000 had an oxbow with slightly higher amplitude. The difference may account for the reversed trend to higher weld line strength of this blend, Fig. 3. The weld line in the blend with PVC molecular weight of 141,000 could not be

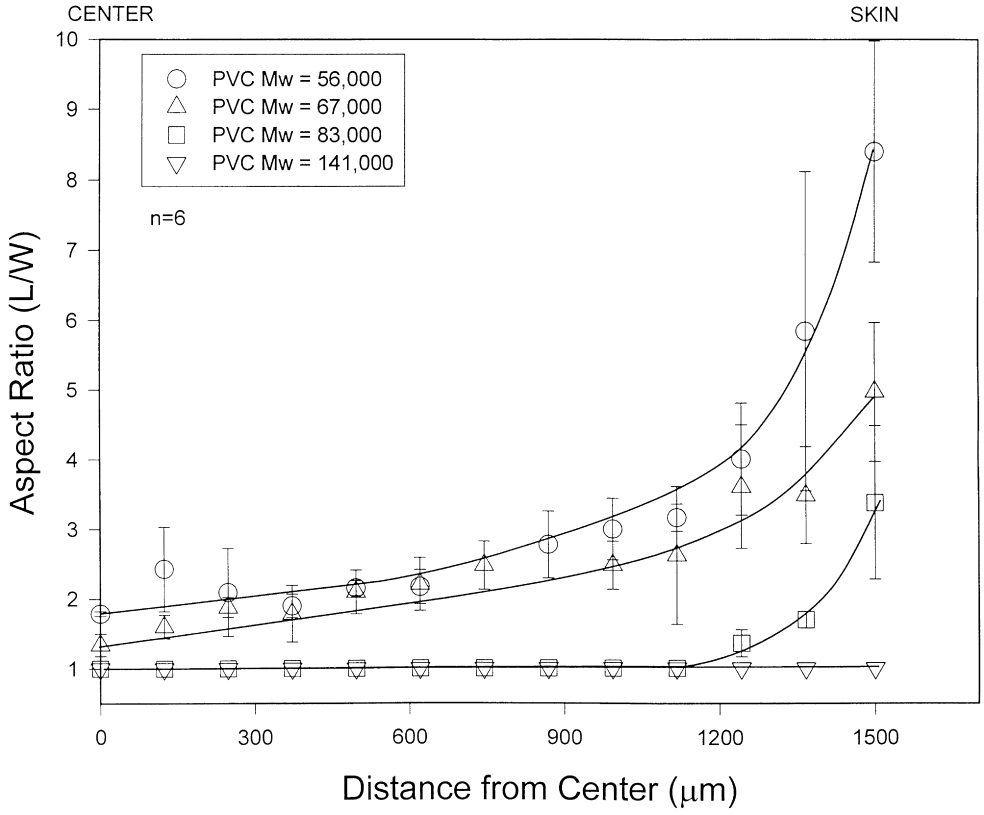

Fig. 5. Aspect ratio of PVC domains as a function of position along the weld line.

distinguished from the bulk, and therefore the precise weld line profile could not be determined.

The weld line was visible in most of the blends because the phase morphology in a region approximately 100 μm on either side of the weld line differed from the bulk morphology. Elongated PVC domains at the weld line acted as markers for the weld line profile. The exception was the blend with 141,000 molecular weight PVC in which the particles were spherical at the weld line. In contrast to the bulk, where shear flow dominated, the material in the weld line had undergone elongational flow at the fountain flow front. This was the same flow field that created the skin, and coincidentally the total thickness of the weld line was approximately two times the thickness of the skin. The orientation of the PVC domains followed the curvature of the weld line.

A region near the skin, where the weld line was oriented perpendicular to the injection direction, was chosen to illustrate the effect of PVC molecular weight on the morphology. Magnified views in Fig. 4 show highly elongated domains of the PVC with molecular weight 32,000, Fig. 4(b). The elongation decreased markedly as the PVC molecular weight increased from 32,000 to 83,000, Fig. 4(c)–(e). The PVC with molecular weight 141,000 was dispersed as spherical primary particles and aggregates of primary particles, Fig. 4(f).

Examination of the PVC domains at other positions along the weld line revealed a gradual increase in the aspect ratio from the center to the edge. This reflected the time the material had spent in the elongational flow. The material at the center had just entered the elongational flow field and had not been deformed to the same extent as the material near the skin. The gradient in PVC domain shape is shown in Fig. 5. In the center, where the PVC domains had just entered the elongational flow field, the aspect ratio was the same as in the bulk. The slight particle elongation in the center was probably induced into the bulk by the elongational flow at the gate. The aspect ratio at the center was approximately 2 for low molecular weight PVC, and decreased to 1 (spherical domains) as the molecular weight increased. The aspect ratio gradually increased from the center to the skin. For 56,000 molecular weight PVC, the aspect ratio increased from 2 at the center to 8–10 in the skin. The gradient became less severe as the molecular weight increased. For 83,000 molecular weight, the particles were spherical through most of the weld line cross section and reached an aspect ratio of only about 3 in the skin. For the highest molecular weight, 141,000, the spherical PVC domains across the entire cross section were indistinguishable from those in the bulk, however the location of the weld line was identifiable by the small v-notches visible at the surface.

3.3. Fractography

The fracture path typically followed the weld line.

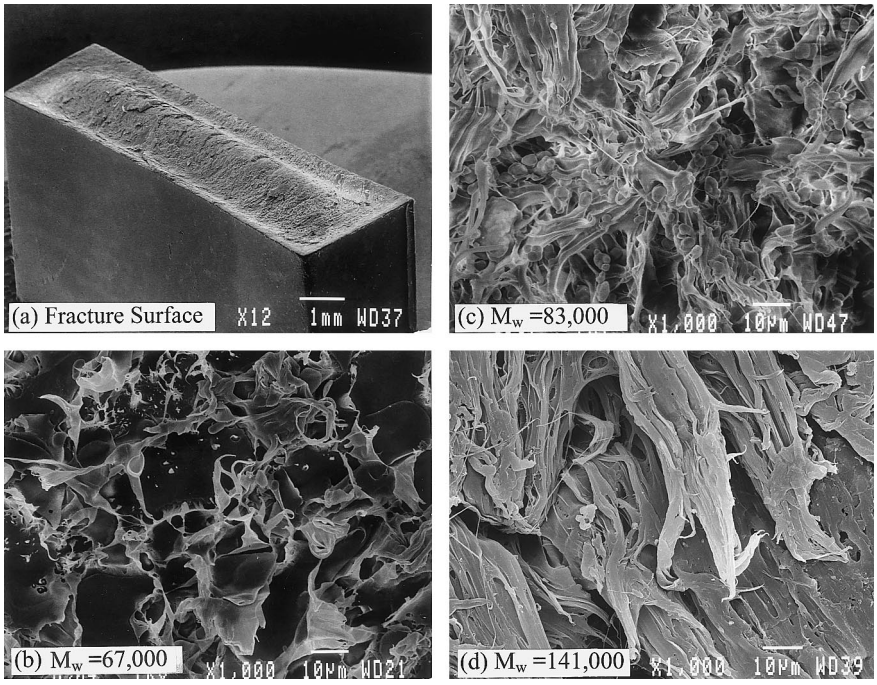

Fig. 6. (a) Typical fracture surface of the low molecular weight PVC blend showing the trough of the weld line where fracture initiated and magnifications of the initiation site for (b) PVC $M_w = 67,000$; (c) PVC $M_w = 83,000$; and (d) PVC $M_w = 141,000$.

Macroscopically, the two fracture surfaces were not the same. The oxbow shape created one surface with a ridge in the center and a matching surface with a center valley. Fractography was performed on the surface with the ridge, Fig. 6(a). In all cases, initiation occurred in the trough that surrounded the center ridge of the weld line. The region with the highest degree of fibrillation, indicating the region of slowest crack growth, identified the fracture initiation site. This was usually close to one end. The size of the initiation site depended strongly on PVC molecular weight. For low molecular weights, a small initiation site occupied less than 5% of the trough. The site was approximately 400 μm long and the width of the trough, about 300 μm. The HDPE on the remainder of the fracture surface was almost undeformed. With increasing PVC molecular weight, the initiation site lengthened as the width remained constant at about 300 μm. The length of the initiation site for intermediate molecular weights approached 10% of the trough, or roughly 900–1200 μm. For the highest molecular weight, 141,000, the initiation site extended over 20% of the trough. The remainder of the fracture surface of lower molecular weight PVC blends indicated brittle fracture. For the higher PVC molecular weights, the entire fracture surface had ductile features, however to a lesser extent than the initiation site.

Magnifications of the fracture initiation site are shown in Fig. 6(b)–(d). The blend with 67,000 molecular weight PVC exhibited disk-shaped PVC domains separated by a small amount of matrix material. The matrix material was fibrillated around the PVC domains but there was no visible deformation of the PVC phase. As the PVC molecular weight increased, and the aspect ratio of the disk-shaped particles decreased, the amount of matrix between the domains and the amount of matrix fibrillation at the fracture initiation site increased. In the blend with spherical domains of the highest molecular weight PVC, the matrix was highly drawn.

Macroscopic views of the region directly below the fracture plane are shown in Fig. 7(a)–(c). In the low molecular weight blends, fracture occurred along the weld line with no subsurface deformation and hence the weld line profile was clearly evident. As the molecular weight increased to 83,000, the fracture surface showed some distortion of the weld line profile. The 141,000 molecular weight blends fractured with considerable deformation on a plane perpendicular to the stress at the site of the weld line, however the weld line profile was not evident.

Higher magnification of the region directly below the initiation site is shown in Fig. 7(d)–(f). With low molecular weight PVC, no damage was observed below the fracture surface. As the PVC molecular weight increased to 83,000 and the PVC particles approached spherical, sub-surface damage was observed in the weld line. A damaged layer of cavitated HDPE surrounding undeformed PVC particles extended a distance of approximately 20–40 μm, incorporating a depth equivalent to 4–8 PVC domains, below the fracture plane. This indicated that the PVC debonded and was not load bearing after yield. This damage zone extended along the entire weld line but was deepest at the initiation site. For the highest PVC molecular weight, the thickness of the damaged region was several hundred microns.

Regardless of the PVC molecular weight, fracture

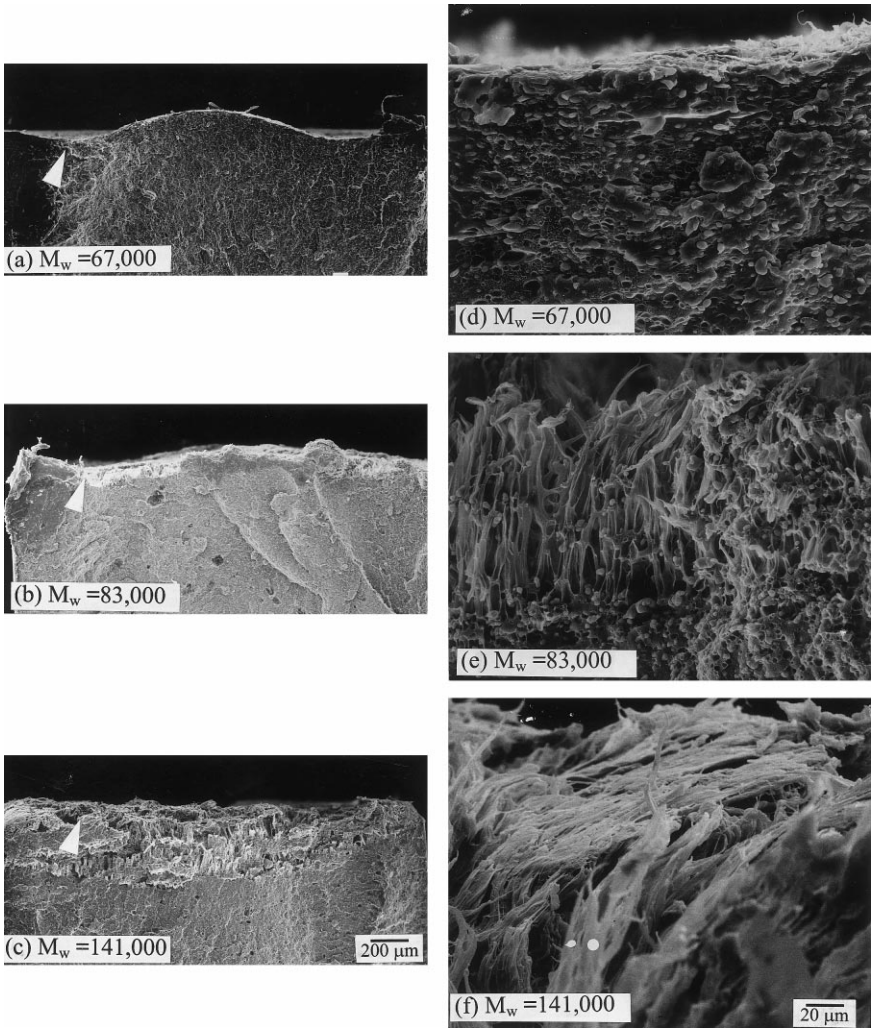

Fig. 7. Macroscopic views of the morphology below the fracture plane: (a) PVC $M_w = 67,000$; (b) PVC $M_w = 83,000$; and (c) PVC $M_w = 141,000$. The arrows indicate the fracture initiation site. Higher magnification of the morphology below the initiation site: (d) PVC $M_w = 67,000$; (e) PVC $M_w = 83,000$; and (f) PVC $M_w = 141,000$.

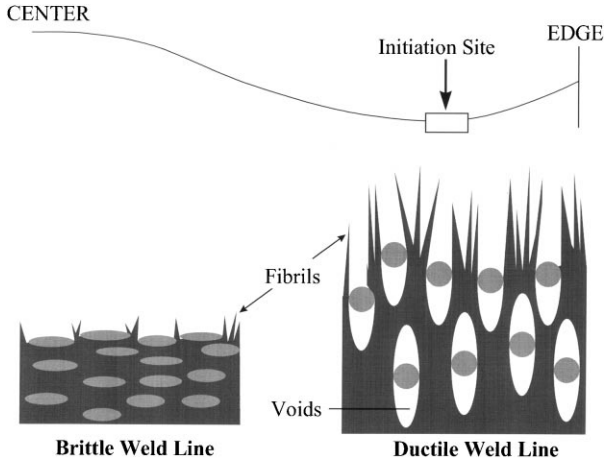

Fig. 8. Schematic representation of the deformation at the fracture initiation site for weak (low molecular weight PVC) and strong (high molecular weight PVC) weld lines.

initiated where the weld line and the elongated PVC particles were oriented perpendicular to the applied stress. A schematic representation of the deformed morphology at the initiation site is presented for low and high molecular weight PVC in Fig. 8. With low molecular weight PVC, fracture initiated at the highly elongated PVC domains by drawing out of the small amount of matrix material between the PVC domains. If the particles were spherical, as with the high molecular weight PVC, there was more matrix material between the particles in the weld line. The increased amount of load bearing matrix facilitated the development of a damage zone below the weld line.

The deformation and fracture processes at the weld line are seen as follows: The matrix yielded around the PVC particles with concurrent debonding from the particles. As the matrix began to draw, cavities opened up around the particles. However, if there was not enough matrix material between PVC domains to support the draw stress (low PVC molecular weight), the weld line fractured. When enough

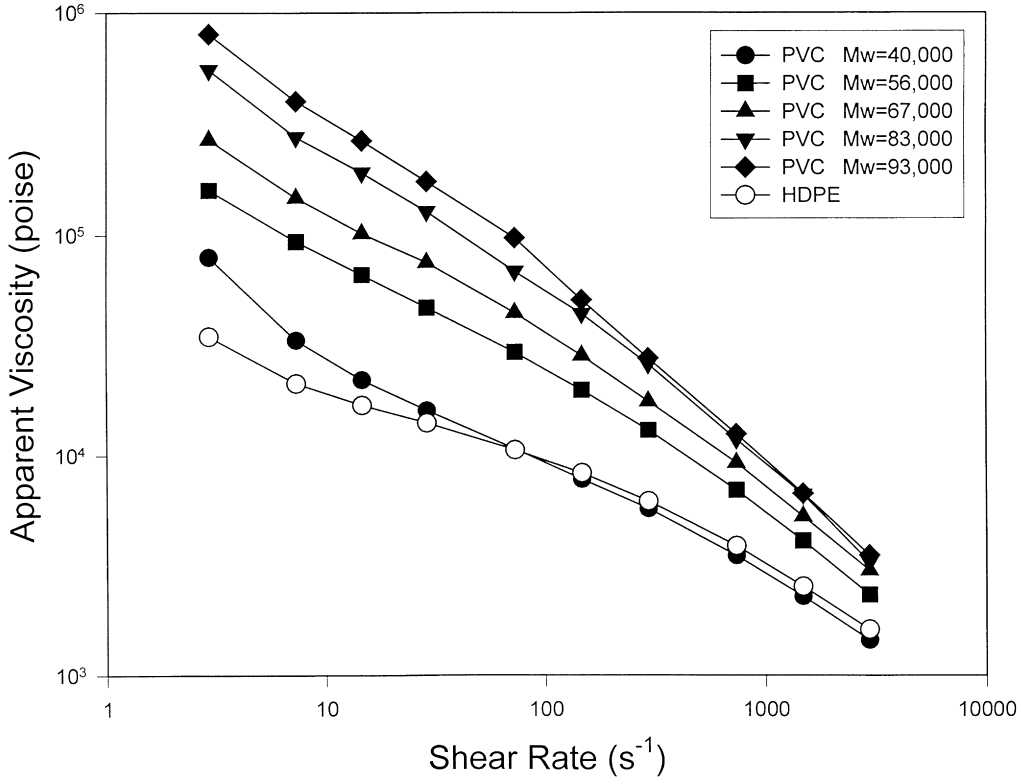

Fig. 9. Apparent viscosity versus shear rate for several PVC molecular weights and HDPE.

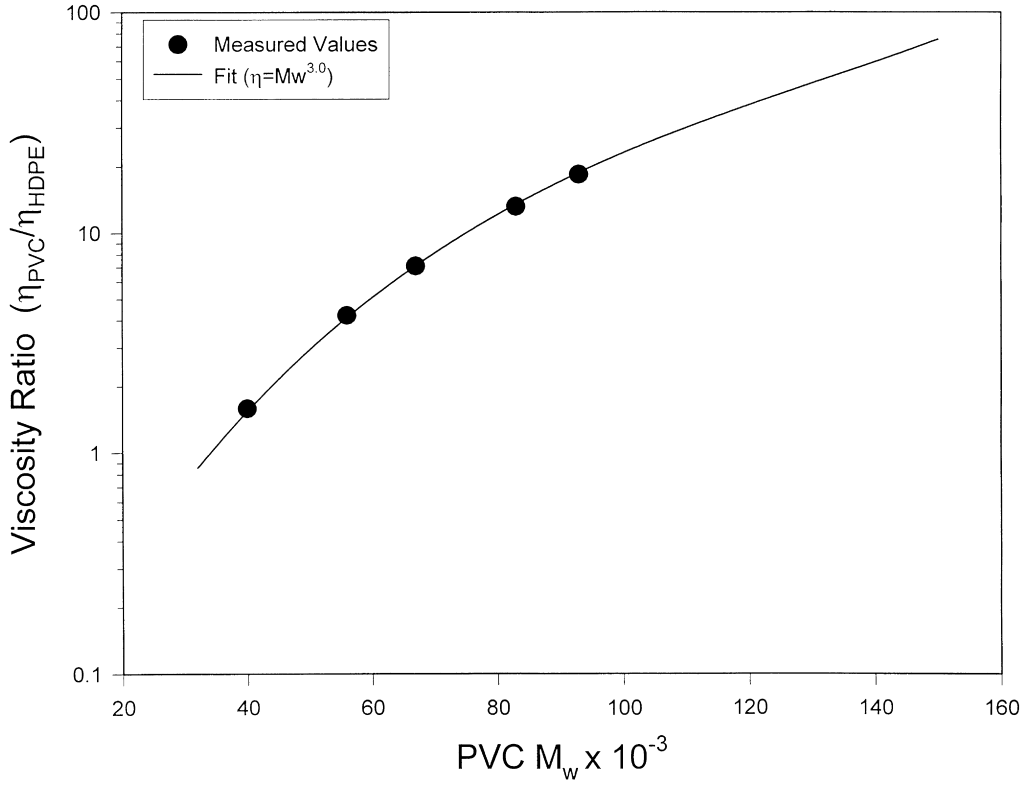

Fig. 10. Effect of PVC molecular weight on the viscosity ratio.

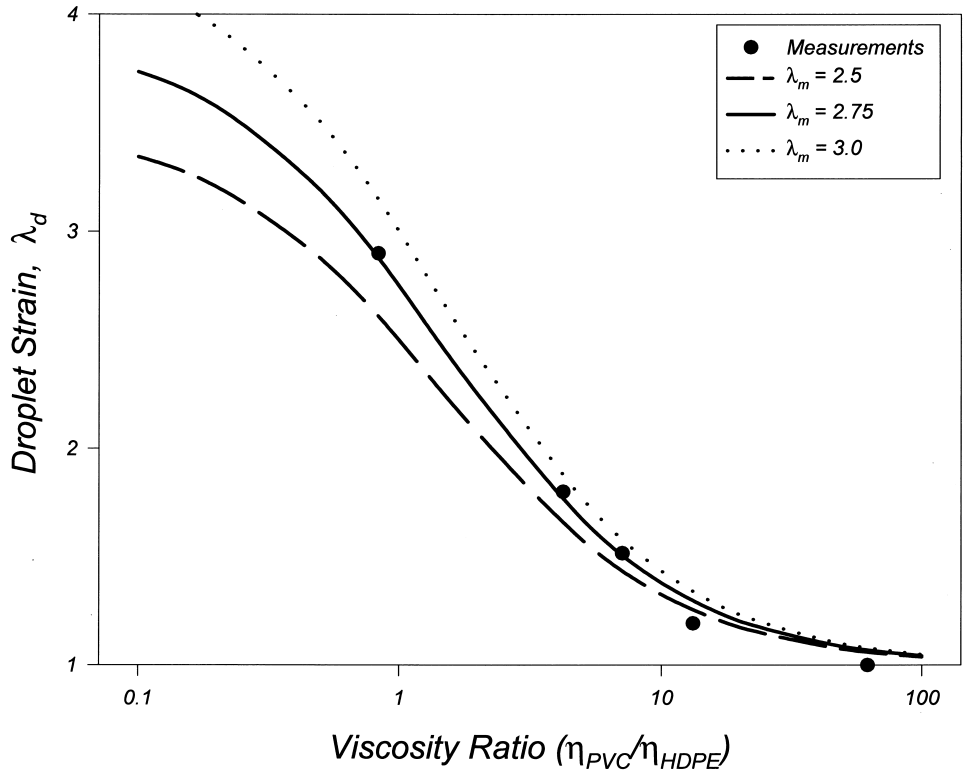

Fig. 11. Comparison of measured PVC droplet strain at the initiation site with droplet strain calculated from droplet deformation theory as a function of viscosity ratio. Three matrix strains are shown with the best fit of $\lambda_m = 2.75$.

matrix existed between the particles (high PVC molecular weight), the drawn fibrils between the PVC particles strain hardened and carried the load. Because there was enough load-bearing material to support the matrix draw stress, yielding and cavitation propagated away from the initiation site. This increased the damage zone size and correspondingly increased the fracture strain. The local draw ratio of the yielded material in the weld line continued to increase as the damage zone grew, and fracture occurred when the fibrils reached the fracture strain of the matrix and a critical void formed. Except for the highest PVC molecular weight, fracture followed the oxbow profile.

3.4. Model for PVC domain shape

The shape of the PVC domains in the weld line was modeled by considering the elongational flow field at the weld line and the rheological properties of the components. For simplicity, a Newtonian approach to droplet deformation was used to describe the shape of the dispersed PVC phase in the elongational flow field. From the classic Taylor droplet deformation theory the droplet strain, λ_d, is calculated from the matrix strain, λ_m, and the viscosity ratio of the components ($p = \eta_{PVC}/\eta_{HDPE}$) [13–15]

$$\lambda_d = \frac{5}{2p+3}(\lambda_m - 1) \quad (1)$$

Although Eq. (1) applies to Newtonian fluids undergoing small strains, it has been found to be valid for viscoelastic fluids with λ_d of over 600% [15,16]. If Eq. (1) is valid, the experimental dependence of λ_d on p should be described by a unique value of λ_m.

For convenience, p was calculated from shear viscosities instead of elongational viscosities. The viscosities, measured at 200°C to match the melt temperature during molding, are depicted in Fig. 9. In all cases, the PVC was at least as viscous as the HDPE and as expected the PVC viscosity increased with molecular weight. The viscosity ratio, p, is presented as a function of PVC molecular weight in Fig. 10. These ratios were calculated for a shear rate of $10\ s^{-1}$. This would seem too low for injection molding, however because in general elongational viscosities are much less "strain thinning" than shear viscosities, a low shear rate was deemed acceptable [17]. The curve is a fit of the data based on a third power dependence of viscosity on molecular weight. Due to the strong dependence of viscosity on the molecular weight for entangled melts [17], the viscosity ratio varied by almost two orders of magnitude in this molecular weight range. Therefore, according to Eq. (1), λ_d should have a strong dependence on the molecular weight.

Rather than attempting to measure the droplet strain in the melt during molding, the PVC particle strain was calculated from the measured aspect ratio (l/w) at the trough where

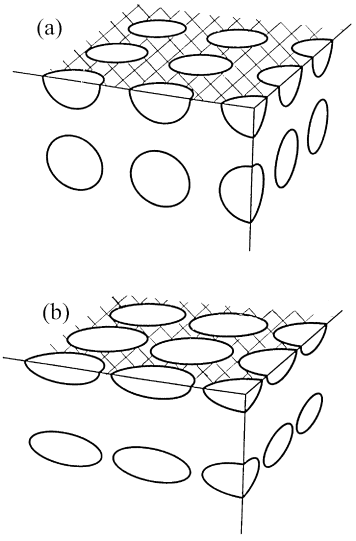

Fig. 12. Schematic comparison of the amount of load bearing matrix in the fracture plane for: (a) spherical particles; and (b) disk-shaped particles.

fracture initiated. The trough was close to the skin where rapid solidification should have preserved the melt morphology. Consistent with the observed symmetrical disk-shaped domains at the weld line, the calculation assumed that the droplet underwent equi-biaxial strain and therefore $\lambda_d = (l/w)^{1/3}$.

The droplet strain, λ_d, is plotted versus the viscosity ratio, p, in Fig. 11. The solid line is a fit of Eq. (1) with $\lambda_m = 2.75$. The fit was unexpectedly good considering that the theory is for Newtonian fluids undergoing small strains at low strain rates. The measured values for high molecular weight PVC were slightly lower than the curve. This may have been caused by higher melt elasticity. The fit indicates that for any viscosity ratio, p, the droplet strain, λ_d, in the trough of the weld line can be predicted using Eq. (1) with $\lambda_m = 2.75$.

3.5. Prediction of weld line strength

The transition from brittle to ductile weld lines was predicted from the shape of the PVC domains. An approach based on the well known ductile to brittle transition of filled polymers was used [18–20]. The approach assumes that the particles are debonded from the matrix and not load bearing. Therefore, the amount of load bearing matrix in the cross section and the strain hardening characteristics of the matrix control the ductile to brittle transition. To determine the amount of load bearing matrix in the weld line, a cubic lattice of particles was assumed and the area of matrix in the plane through the midpoints of the particles was determined. The cross sectional area of the HDPE matrix, A_{HDPE}, is a function of the volume fraction of filler

$$A_{HDPE} = (1 - \beta V_f^{2/3}) \quad (2)$$

where V_f is the volume fraction of PVC and β is a geometric constant based on the particle shape. For spherical particles,

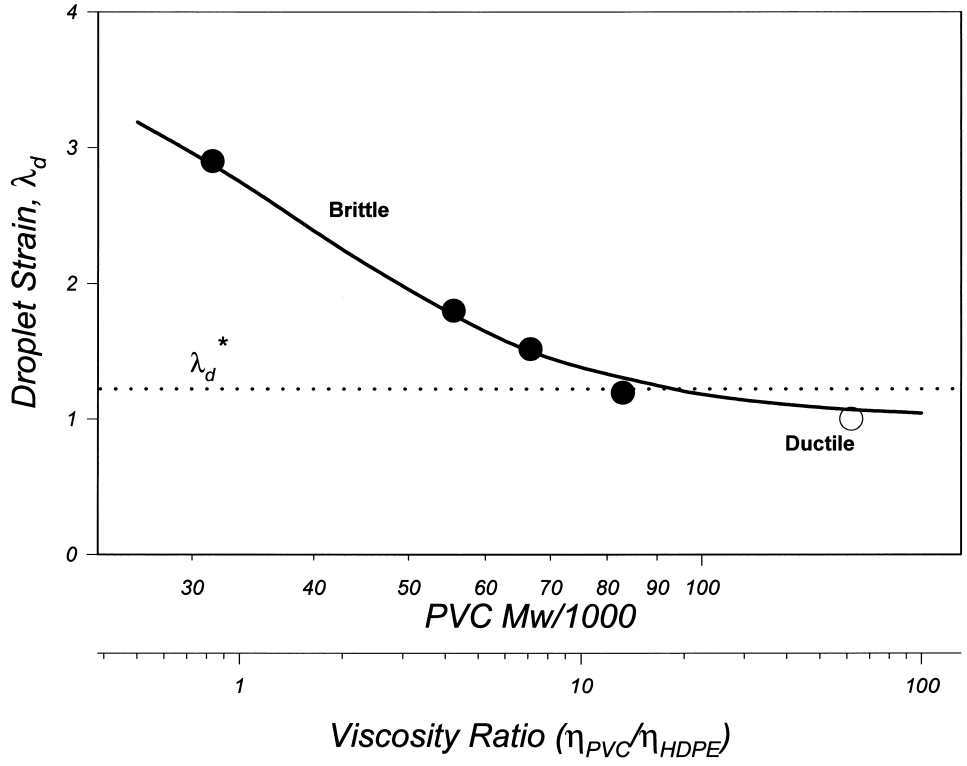

Fig. 13. Comparison of calculated and measured PVC droplet strain with the critical value for a ductile weld line. Filled circles indicate a brittle weld line and an open circle indicates a ductile weld line.

$\beta = (9\pi/16)^{1/3}$. For aligned disk-shaped particles, the matrix area was calculated in the plane through the long axis of the disks. In this case, β, the geometric constant, becomes $\lambda_d^2(9\pi/16)^{1/3}$. The decrease in matrix area for constant V_f as λ_d increases is shown schematically in Fig. 12.

Considering that the crack propagates in the plane that contains the long axis of the particles, the brittle to ductile transition can be determined by combining the calculation of matrix area with the mechanical properties of the matrix. Following the approach for filled polymers, the ductile to brittle transition is related to the draw stress and the fracture stress of the matrix material [20]. Assuming that the ultimate strength of the fibrils between particles is the same as that of the unfilled polymer, σ_f, the fracture stress of the weld line, $\sigma_{f,weld}$, is the product of the initial cross sectional area of the matrix and the fracture stress of the matrix,

$$\sigma_{f,weld} = A_{HDPE}\sigma_f \tag{3}$$

If $\sigma_{f,weld}$ is higher than the draw stress of the matrix, σ_d, the weld line will yield and be ductile. The ductile to brittle transition occurs when $\sigma_{f,weld}$, equals the draw stress of the matrix, σ_d,

$$\sigma_d \cong \sigma_{f,weld} \tag{4}$$

Combining Eqs. (2)–(4) with the factor β for disk-shaped domains and solving for λ_d, the critical droplet strain, λ_d^*, at the ductile to brittle transition for composition V_f is

$$\lambda_d^* = \left(\frac{1 - \dfrac{\sigma_d}{\sigma_f}}{\left(\dfrac{9\pi}{16}\right)^{1/3} V_f^{2/3}} \right)^{1/2} \tag{5}$$

The measured draw stress and fracture stress of the HDPE matrix were 80 and 240 MPa, respectively, and the PVC volume fraction was 0.225. Inserting these values into Eq. (5) gave λ_d^* of 1.24. If λ_d were larger than this, the weld line would be brittle.

The critical λ_d^* from Eq. (5) is compared with the experimental λ_d values and λ_d calculated from Eq. (1) in Fig. 13. The intersection of the λ_d curve with λ_d^* identifies a minimum PVC molecular weight of 97,000 (or a viscosity ratio of 21) for weld lines of this blend composition to be ductile. The correlation is excellent. Blends with PVC molecular weights well below 97,000 fractured in a brittle manner. With a molecular weight of 83,000, approaching the critical value of 97,000, damage occurred along the entire weld line and the fracture stress almost reached the yield stress. With a molecular weight of 141,000, above the critical value, the weld line yielded and fractured during neck formation.

4. Conclusions

In summary, elongation of the PVC phase at the weld line was found to be the cause of weak weld lines. Increasing the PVC molecular weight increased the viscosity ratio and consequently the elongation of the PVC phase decreased. A Taylor analysis modeled the elongation of the PVC phase surprisingly well. The ductile to brittle transition was determined as a function of the PVC domain shape using a modified Nielsen approach. The approach predicted a maximum biaxial strain of the PVC particles of 1.24 before the matrix area would be insufficient to support the draw stress and the ductile to brittle transition would occur. To achieve a particle strain less than 1.24, a viscosity ratio greater than 21 would be required for the blend composition studied.

Acknowledgements

The authors would like to thank Dave Poledna and Phil Bak at Geon for synthesizing some of the resins, and Juan Rodriguez at Geon for his assistance in blending the materials. The financial support of The Geon Company is gratefully acknowledged.

References

[1] Hagerman E. Plast Eng 1973;:67.
[2] Robeson LM. Polym Eng Sci 1982;22:1001.
[3] Fisa B, Favis BD, Bourgeois S. Polym Eng Sci 1990;27:241.
[4] Meddad A, Fisa B. Polym Eng Sci 1995;35:893.
[5] Utracki A. Two phase polymer systems, New York: Hanser, 1991.
[6] Grace H. Chem Eng Commun 1982;14:225.
[7] Thamm RC. Rubber Chem Technol 1977;50:24.
[8] Rabinovitch EB. J Vinyl Technol 1982;4:62.
[9] Summers JW, Rabinovitch EB. J Vinyl Technol 1991;13:54.
[10] Bazhenov S, Li JX, Hiltner A, Baer E. J Appl Polym Sci 1994;52:243.
[11] Dairanieh S, Haufe A, Wolf HJ, Mennig G. Poly Eng Sci 1996;36:2050.
[12] Mennig G. Kunstst—Ger Plast 1992;82:235.
[13] Taylor GI. Proc R Soc London Series A 1932;138:41.
[14] Taylor GI. Proc R Soc London Series A 1934;146:510.
[15] Delaby B, Ernst Y, Germain R. Muller. J Rheol 1994;38:1705.
[16] Kalb B, Cox G, Manley RSJ. J Coll Interf Sci 1981;83:286.
[17] Macosko CW. Rheology principles, measurements and applications, New York: VCH, 1994.
[18] Nielson LE. J Compos Mater 1967;1:100.
[19] Nielson LE. J Appl Polym Sci 1966;10:97.
[20] Bazhenov JX, Li A, Hiltner E. Baer. J Appl Polym Sci 1994;52:243.